Optimal, Real-Time Monitoring of Particle Size Distribution in a Fluidized Bed

A novel method for tracking particle size distribution dynamics in a fluidized bed yields on-line, real-time measurements of particle size distribution that are representative of actual conditions. These measurements are somewhat corrupted with noise (random error), however, and are available to the computer only at discrete time intervals. An optimal filtering algorithm combines the measurements with predictions from an idealized dynamic model to yield particle size distribution estimates that are not only on-line and real-time, but also virtually continuous and well-behaved.

D. J. Cooper
Department of Chemical Engineering
University of Connecticut
Storrs, CT 06268

D. E. Clough
Department of Chemical Engineering
University of Colorado
Boulder, CO 80309

SCOPE

We have developed an experimental method for obtaining on-line, real-time particle size distribution measurements in a fluidized bed. In this method, a continuously flowing stream of sample particles is drained from the fluidized bed. The sample particles are pneumatically entrained, blown through the object plane of an optical array spectrometer particle size analyzer, and then channeled back to the freeboard region of the fluidized bed. The analyzer automatically sizes individual particles as they cut the object plane, and transmits the data to a process computer system. The computer collects the incoming data and resolves it to yield overall bed particle size distribution measurements once every 60 s.

This method produces on-line, real-time particle size distribution measurements that are representative of actual conditions in the bed. These measurements are somewhat corrupted with random error (noise), however, and they are available only at discrete intervals in time. For advanced monitoring and control applications, it is desirable to have measures of pertinent process parameters such as fluidized bed particle size distribution that are not only on-line and real-time, but also continuous in time and well-behaved (little random error).

Optimal estimation theory provides a mathematical framework for obtaining continuous, well-behaved estimates from noisy, discrete-time measurements. This work details the application of optimal estimation theory to our method of particle size distribution measurement. An optimal filtering algorithm is derived that can predict in real time a virtually continuous particle size distribution between on-line measurements, and then can update this predicted distribution whenever new measurements become available. After reviewing the experimental method for obtaining the on-line measurements, we present results from an experimental demonstration in which we obtain on-line, real-time, continuous and well-behaved estimates of overall bed particle size distribution throughout the course of a significant distribution transient.

CONCLUSIONS AND SIGNIFICANCE

Particle size distribution is fundamental to the performance and operation of fluidized bed processes. An accurate, on-line, real-time, and well-behaved measure of particle size distribution would therefore contribute to improved process knowledge, and subsequently to improved process performance and operation.

Such a measure has value both in the laboratory and in the chemical process industry. For instance, it would

prove valuable in the on-line estimation of other fundamental fluidized bed parameters that are difficult to measure. Some examples include the estimation of minimum fluidization velocity while operating above the minimum, the estimation of the elutriated fines distribution and mass flow rate, the estimation of bubble size and rise velocity during operation, and the estimation of the reaction rate in a mass-transfer-limited reaction. When this technology for overall bed particle size distribution measurement matures, it will even provide the information necessary for particle size distribution itself to be controlled.

We have demonstrated in this work that on a laboratory scale we can obtain overall fluidized bed particle size distribution estimates that are on-line, real-time, continuous, and well-behaved. An optimal filtering algorithm produces these estimates by combining predictions from an idealized dynamic model with measurements that are on-line and real-time, but available only at discrete time intervals and somewhat corrupted with random error (noise). Further, the optimal monitoring capabilities have been experimentally demonstrated to perform satisfactorily throughout the course of a significant particle size distribution transient.

Introduction

Advanced control methods require that current and accurate measures of the important process parameters be available for use by the on-line process computer. When considering the operation of fluidized beds, one parameter of fundamental importance is particle size distribution (PSD). Particle size distribution affects fluidization behavior, transport and kinetic properties in the bed, and process considerations for operation. Many factors affect PSD, including solids feed, solids discharge, fines elutriation, particle growth (e.g., agglomeration, deposition), and particle shrinkage (e.g., attrition, reaction).

We have developed and demonstrated an experimental method for tracking overall PSD in a fluidized bed (Cooper and Clough, 1985a). In this method, a continuously flowing stream of sample particles drains from a well-mixed fluidized bed into a pneumatic liftpipe where the particles become entrained in a rapidly moving transport medium of air. The sample particles are elevated in the liftpipe and channeled so that they blow through a sample measurement chamber and back to the freeboard region of the fluidized bed. This sample system thus completes a continuously flowing, closed-loop pattern.

In passing through the sample measurement chamber, the particles cross the object plane of an optical array spectrometer particle size analyzer. The analyzer automatically sizes individual particles as they cut the object plane, and it transmits the size data to a process computer. The process computer collects individual particle size data for 25,000 particles over a period of 60 s and resolves the data as an overall bed PSD presented mathematically as a mass-fraction probability density function. The method thus yields one PSD measurement per minute based on the individual sizing of 25,000 sample particles.

The on-line measurements, made automatically and with little time delay after sampling, are representative of actual conditions in the bed. The PSD measurements are somewhat corrupted with random error, however, with the measurement noise increasing toward the large-particle range of the particle size analyzer. Also, the maximum frequency at which on-line measurements can be made is only once every 60 s. Though such a time interval allows the proper tracking of even the most dramatic of distribution dynamics, a continuous measure of PSD is of more value in advanced control applications.

An optimal filtering algorithm can produce on-line, real-time, virtually continuous, and well-behaved estimates of PSD. The estimates are based on measurements of PSD that are on-line and real-time, but that are somewhat corrupted with random error (noise) and are available to the computer only at discrete intervals in time. The filtering algorithm, derived from optimal estimation theory, produces the improved estimates by minimizing a least-squares error criterion that combines incoming measurements with predictions from an idealized dynamic model. The theory for filtering noisy but continuous fluidized bed PSD measurements has been developed for the general case and demonstrated via off-line simulation studies (Cooper and Clough, 1985b).

In this work we detail the application of the general PSD filtering theory to the specific application of our on-line PSD measurement method. We begin by tailoring the general optimal filtering algorithm for the case where on-line PSD measurements are made at discrete time intervals. Such a filtering algorithm must yield a virtually continuous real-time prediction of PSD between each on-line measurement, and a filtered update of the prediction at the time of each measurement. We next review the experimental apparatus and procedures used to obtain the on-line PSD measurements. We then present results from an experimental demonstration. On-line, real-time, continuous, and well-behaved estimates of the overall PSD were determined in a large-particle, sand-air fluidized bed throughout the course of a significant distribution transient. We conclude with a discussion of the work.

Theoretical Development

Dynamic mixing model

To make the application of optimal estimation theory to our method of PSD measurement most illustrative, we desired a significant PSD transient during the experiment. We achieved this transient via a PSD "dilution." As illustrated in Figure 1, a PSD dilution entails loading the fluidized bed with an initial charge of silica sand of known PSD, $P_b(d, 0)$, and loading the overhead fresh feed bin with sand of a different known PSD, $P_0(d)$. The dilution is then accomplished by injecting the fresh feed into the fluidized bed at a constant rate. Particles leave the bed either by spilling through the overflow pipe or by entrainment in the fluidizing air. In this demonstration no reaction occurred, and since the duration of the experiment was short, we assumed negligible attrition. With the further assumptions of constant expanded bed density and volume, the following general relation can be

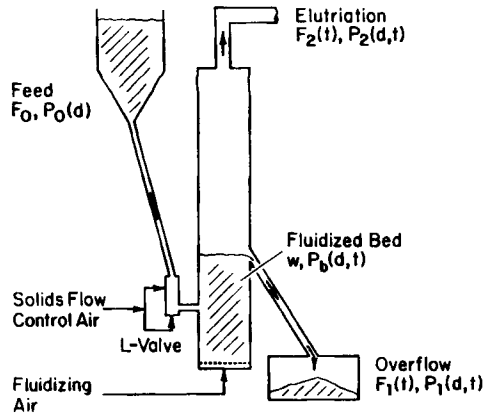

Figure 1. Fluidized bed, schematic diagram.

derived for spherical particles of diameter d_i:

$$w\frac{dP_b(d_i,t)}{dt} = F_0 P_0(d_i) - F_1(t)P_1(d_i,t) - F_2(t)P_2(d_i,t) \quad (1)$$

with the requirement that at all times, the PSD, presented mathematically as a mass-fraction probability density function, be normalized such that:

$$\int_0^{d_{\max}} P_b(s,t)\,ds = 1.0 \quad (2)$$

The form of the dynamic model can be recast by introducing an elutriation constant (Levenspiel et al., 1968; Weimer and Clough, 1980; Wen and Chen, 1982) of the form:

$$K(d,t) = \frac{F_2(t)P_2(d,t)}{w\,P_b(d,t)} \quad (3)$$

and by specifying that the fluidization velocity is high enough (approximately three times minimum fluidization or greater such that:

$$P_1(d,t) \approx P_b(d,t) \quad (4)$$

Substitution of Eqs. 3 and 4 into Eq. 1 and rearranging yields a fluidized-bed dynamic model of the form:

$$\frac{dP_b(d_i,t)}{dt} = \alpha(d_i,t)P_b(d_i,t) + \beta(d_i) \quad (5)$$

where

$$\alpha(d_i,t) = -K(d_i,t) - \frac{F_1(t)}{w} \quad (6)$$

and

$$\beta(d_i) = \frac{F_0 P_0(d_i)}{w} \quad (7)$$

The fluidized bed PSD, $P_b(d,t)$, is continuous over particle diameter. A finite–difference approximation, however, results in a spatial domain that can be represented as a vector of N discrete particle diameters, i.e.

$$X(t) = \begin{bmatrix} P_b(d_1,t) \\ P_b(d_2,t) \\ \cdot \\ \cdot \\ \cdot \\ P_b(d_N,t) \end{bmatrix} \quad (8)$$

If we also introduce $A(t)$ and B as appropriately defined, spatially discrete vector representations for $\alpha(d,t)$ and $\beta(d)$, respectively, the system of N ordinary differential equations for diameters $0 \le d_i \le d_N$ can be written in matrix notation as:

$$\dot{X}(t) = A(t)X(t) + B \quad (9)$$

Optimal filtering algorithm

We first consider the linear system describing the case where the on-line PSD measurement is continuous in time:

$$\dot{X}(t) = A(t)X(t) + B + U(t) \quad (10a)$$

$$Z(t) = X(t) + V(t) \quad (10b)$$

$$X(t_0) = X_0 + U(t_0) \quad (10c)$$

Here, $Z(t)$ is the spatially discrete PSD measurement vector, assuming continuous PSD measurement for each of the N discrete particle size diameters. Also, X_0 is an a priori estimate vector of the true initial PSD, $X(t_0)$, and the variables $U(t)$ and $V(t)$ are spatially discrete noise vectors representing the uncertainties in the idealized mixing model and the raw on-line measurements, respectively. Both $U(t)$ and $V(t)$ are assumed to be Gaussian-distributed, zero-mean, and white in time with respective covariance matrices:

$$E[U(t)U^T(\tau)] = Q(t)\delta(t-\tau) \quad (11a)$$

$$E[V(t)V^T(\tau)] = R(t)\delta(t-\tau) \quad (11b)$$

The a priori initial PSD estimate, X_0, similarly has a covariance matrix:

$$E[X_0X_0^T] = P_0 \quad (12)$$

Because our system is described by a set of ordinary differential equations, the covariance matrices $Q(t)$, $R(t)$, and P_0, are diagonal in form. That is, all off-diagonal terms in these matrices are zero.

As detailed in the literature (Bryson and Ho, 1975; Sage and White, 1977; Ray, 1981; Cooper and Clough, 1985b), the minimization of a quadratic least-squares error criterion for this system leads to the following pair of linear, simultaneous filter equations:

$$\dot{X}^*(t) = A(t)X^*(t) + P(t)R^{-1}(t)[Z(t) - X^*(t)] \quad (13a)$$

$$\dot{P}(t) = A(t)P(t) + P(t)A(t)^T + Q(t) - P(t)R^{-1}(t)P(t) \quad (13b)$$

with initial conditions:

$$P(t_0) = P_0 \tag{13c}$$

$$X^*(t_0) = X_0 \tag{13d}$$

where $X^*(t)$ is the optimal (minimum least-squares error) PSD estimate N-vector, and $P(t)$ is the $N \times N$ optimal estimate error covariance matrix.

In our experimental method, the on-line PSD measurements are not made continuously, but are made at discrete time intervals. The discrete measurement model is more properly described as:

$$Z(t_k) = X(t_k) + U(t_k) \tag{14}$$

where t_k is the time at the kth successive measurement. The discrete measurement error covariance exists only at the time of measurement and is expressed in the form:

$$R(t) = R(t_k)\delta(t - t_k)\Delta t_k \tag{15}$$

Here, Δt_k is the time interval between the discrete measurements, and δ is the Dirac delta function.

Substitution of Eq. 15 into Eqs. 13a–d yields two sets of discrete measurement filter equations. The first set of filter equations is applicable between each on-line PSD measurement, such as times $t_{k-1} < t < t_k$. In this time interval, when $t \neq t_k$, then $R(t) = 0$. The resulting prediction equations are used to compute a virtually continuous optimal estimate of fluidized bed PSD between each raw on-line measurement:

$$\dot{X}^*(t) = A(t)X^*(t) \tag{16a}$$

$$\dot{P}(t) = A(t)P(t) + P(t)A(t)^T + Q(t) \tag{16b}$$

The second set of filter equations is applicable at the time of each on-line measurement. At measurement time $t = t_k$, then $R(t) = R(t_k)\Delta t_k$. We denote $X^*(t_k^-)$ as the optimal real-time PSD estimate computed by prediction equation 16a at measurement time t_k. Similarly, $P^*(t_k^-)$ is the optimal real-time estimate error covariance computed by prediction equation 16b at t_k. Substitution of Eq. 15 into Eqs. 13a–d for this case, after considerable manipulation (Ajinkya, 1975), yields the resulting update equations used to compute the optimal filtered estimate of PSD at discrete time measurement $Z(t_k)$:

$$X^*(t_k^+) = X^*(t_k^-) + P(t_k^-) \cdot (P(t_k^-) + R(t_k)\Delta t_k)^{-1}[Z(t_k) - X^*(t_k^-)] \tag{17a}$$

$$P(t_k^+) = P(t_k^-) - P(t_k^-) \cdot (P(t_k^-) + R(t_k)\Delta t_k)^{-1}P(t_k^-) \tag{17b}$$

Eqs. 16a, b are thus integrated forward in real time to predict the optimal real-time estimate of overall bed PSD between on-line measurements, and Eqs. 17a, b are used to compute the filtered update of PSD based on the incoming on-line measurement and the real-time predicted estimate.

Experimental

Apparatus

The apparatus used in this demonstration has been detailed elsewhere (Cooper and Clough, 1985a) and is briefly described here. As illustrated in Figure 1, the solids processing fluidized bed consists of a 0.29 m ID clear cast-acrylic cylinder filled to a collapsed depth of 0.5 m with silica sand. Fresh sand is injected midway into the expanded fluidized bed via an L-valve. The expanded bed level is maintained via an overflow pipe that discharges into a sealed overflow bin.

The sampling system, illustrated in Figure 2, is a continuously flowing, closed-loop sampling system. A sample tap is situated so that a continuously flowing sample drains from a point located radially halfway between the center of the bed and the cylinder wall, and vertically halfway between the bottom and the top of the expanded fluidized bed. The sample tap length of 1 m is long enough and the sand sample flow through it of 20 to 25 mm/s is fast enough so that an effective seal-leg exists between the fluidized bed and the pneumatic liftpipe. The pneumatic liftpipe, with a transport medium of air traveling through it at a superficial velocity of 25 m/s, dilutes the sand sample as it elevates it up to the sample measurement chamber. The entrained flow of sample sand is channeled so that it blows through the sample measurement chamber and back to the freeboard of the fluidized bed.

The sample measurement chamber, illustrated in Figure 3, allows the continuously flowing diluted sand sample to remain contained within the sample system, yet permits a clear optical path for sample measurement. Attached to opposing sides of the sample measurement chamber are offset tubes with assemblies that hold and seal two optical windows. A steady flow of purge air, injected in front of each window, blows down the offset tubes and exits into the sample measurement chamber. The optical windows are thus protected from damage by the highly abrasive sand stream and the result is a clear optical path for laser illumination.

The particle size analyzer used in this work is the OAS Optical Array Spectrometer made by Particle Measuring Systems, Inc. More specifically, we have used the OAP-230L,

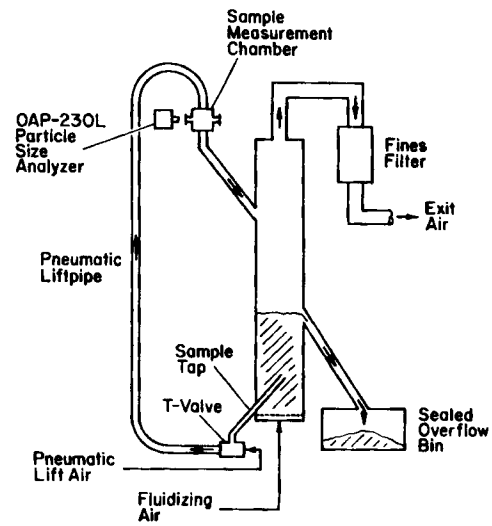

Figure 2. Continuous-flow, closed-loop sample system.

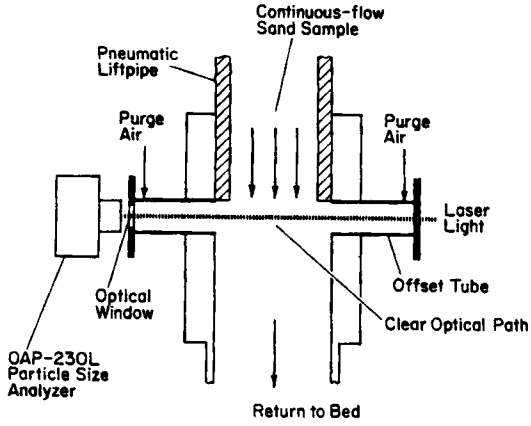

Figure 3. Sample measurement chamber.

which is only the laser measuring probe of the OAS device. The OAP-230L is a laboratory probe that uses optical occultation to measure in one dimension, measuring the maximum diameter of each particle. Optical (or light) occultation can be used with opaque or light-absorbing particles. An incident beam of laser light illuminates particles passing through the object plane of a 30-photodiode string imaging array. Each particle completely blocks the laser light, casting a shadow image onto the imaging array. The size of an individual particle is determined from the number of photodiode elements shadowed. The particle shadow must be focused within the boundary limits of the 30-photodiode string imaging array or the OAP-230L will reject the reading.

The measurement range for our probe is calibrated to be 50–1,500 μm. A specially constructed interface board accepts individual particle size measurement signals from the OAP-230L, latches the data, and holds it until it is read onto the data bus of the laboratory process microcomputer. The process microcomputer collects 25,000 individual particle size counts from the particle size analyzer over the course of one minute, and performs computations that resolve the data as a single PSD measurement in the form of spatially discrete 30-channel histogram.

Procedures

A PSD transient was achieved in our laboratory fluidized bed via a PSD dilution. A PSD dilution entails loading the fluidized bed with sand of a known PSD, and the overhead fresh feed bin with sand of a different known PSD. The dilution is then accomplished by injecting the fresh feed at a constant rate into the fluidized bed via the L-valve. This procedure yields a definite, controllable PSD transient. Total expanded bed height is maintained relatively constant throughout the dilution via the overflow pipe. The fluidization velocity is kept above $3U_{mf}$ (three times the minimum fluidization velocity) throughout the experiment to ensure that the bed remains well mixed.

As the dilution proceeds, a continuously flowing sand sample drains into the closed-loop sample system. The time delay introduced from the time that the particle sample is withdrawn from the bed until the time that it passes through the object plane of the OAP-230L photodiode imaging array is less than 50 s. Particle measurement at this point is virtually instantaneous.

The combination of the OAP-230L particle size analyzer, our interface board, and the process microcomputer is such that this equipment can size about 90,000 individual particles every 60 s when operating at maximum measuring rate. This measurement load consumes the total resources of our microcomputer, however, and other tasks are required of it during operation (e.g., flow rate control, pressure drop monitoring). With this in mind, we designed the software so that it would accept 25,000 particle size counts from the OAP-230L every 60 s. We selected this collection rate as a balance that assures a large enough sample to be statistically representative, yet affords the microcomputer sufficient time to perform other tasks.

After collecting the 25,000 raw particle size counts, the microcomputer software then directs simple data reduction computations to arrive at one PSD measurement. Because of the optics associated with the OAP-230L probe, the raw particle size counts must first be adjusted to account for effective sample area. Effective sample area changes with particle size for two reasons. The first is the depth of field associated with focusing the particle shadow images onto the photodiode imaging array. Larger particles have a larger depth of field and therefore have a larger effective sample depth where their particle shadow image will be successfully focused. This larger effective sample depth increases until, at a particle diameter of about 0.20 mm, physical limitations imposed by the measurement chamber walls are reached.

The second contribution to the effective sample area calculation is due to the fact that larger particles have a smaller effective imaging array width. The smallest particle diameter of 0.05 mm has an effective imaging array width that is thirty times its diameter. At the other extreme, however, the largest particle diameter of 1.50 mm has an effective imaging array width equal to its diameter. Thus, larger particles have a statistically smaller probability of having their shadow image focused within the imaging array boundary limits. This increased probability of rejected readings for larger particles results in an increasing random variation in total raw measurement counts for these sizes. It is this phenomenon which we believe causes increasing random error toward the large-particle range of the OAP-230L observed in our method.

After the raw particle size counts are adjusted to account for effective sample area, the computer then directs computations to transform the population distribution yielded by the OAP-230L particle size analyzer into a mass distribution. This straightforward calculation is performed by assuming spherical particles and uniform particle density. The calculation is performed because a mass-fraction PSD allows for comparison of our on-line PSD measurements with results of a sieve analysis, which also yields a PSD by mass fraction. Finally, the mass distribution is normalized to a proper probability density function, as defined in Eq. 2, yielding a single PSD measurement. A Newton-Cotes trapezoidal integration (Carnahan et al., 1969) is the numerical method employed in the normalization computations.

Computational Details

1. *Linear vs. Nonlinear.* Up to this point, the PSD dilution model has been presented as a linear differential equation with variable coefficients. The optimal filtering algorithm also has been developed for a linear system. Consider that:

$$F_1(t) = F_0 - F_2(t) \tag{18}$$

By assuming spherical particles, $F_2(t)$ can be expressed as (Levenspiel, 1968):

$$F_2(t) = w \int_0^{d_{max}} K(s, t)P_b(s, t)\, ds \tag{19}$$

Substitution of Eqs. 18 and 19 into Eq. 6 yields a form for the dynamic model coefficient:

$$\alpha(d, t) = -K(d) - \frac{F_0}{w} + \int_0^{d_{max}} K(s, t)P_b(s, t)\, ds \tag{20}$$

Because $P_b(d, t)$ appears in the coefficient $\alpha(d, t)$, the dynamic PSD dilution model is actually a nonlinear differential equation. Euler integration (forward difference in time) is a simple numerical integration technique that can be shown to be a successive linearization in time of this nonlinear term. Thus, employing Euler integration for numerical integration enables the use of linear filtering theory.

2. *Parameter Values.* Illustrated in Figure 4 is the initial on-line measurement for the overall fluidized bed PSD, $P_b(d, 0)$. Also shown is the fresh feed PSD, $P_0(d)$. The *a priori* estimate vector of the fluidized bed PSD, X_0, used as the initial condition for the optimal filtered estimate, Eq. 16a, was set equal to spatially discretized $P_b(d, 0)$. Table 1 contains other parameter values used in the demonstration run.

3. *Covariance (Weighting) Matrices.* As can be seen in Figure 5a, measurement noise (random error) increases toward the large-particle range of the particle size analyzer. In contrast, the fine-particle range is relatively well-behaved. To reflect that our confidence in the on-line measurements decreases with increasing particle size (because the measurement error increases with increasing particle size), we assigned a weighting value for the measurement error covariance matrix that increases linearly with particle diameter. We also defined the matrix to be constant over time. The equation we employed to compute this sliding scale for the diagonal terms was:

$$R_{diag}(d_n, d_n, t) = 0.0010 + 0.0033n \tag{21}$$

for $n = 0, \ldots, 30$ and all off-diagonal terms are zero. Because we used the first on-line measurement of fluidized bed PSD,

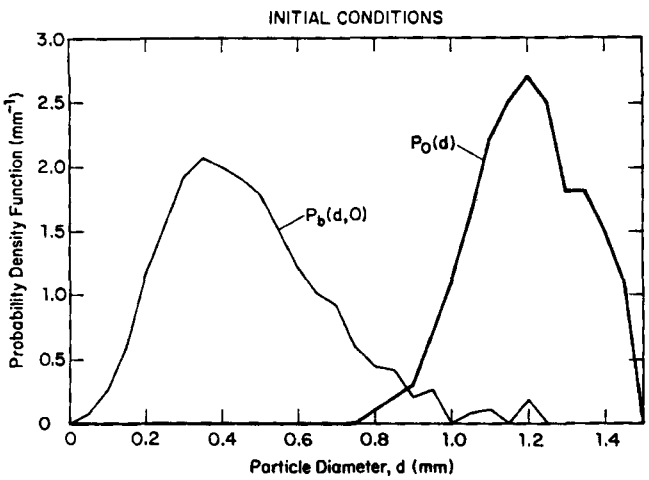

Figure 4. Initial bed and feed particle size distribution.

Table 1. Parameter Values Used in Demonstration

Fresh Feed Rate	$F_0 = 0.045$ kg/s
Fluidized Bed Weight	$w = 45$ kg
Discrete Diameters	0.00, 0.05, 0.10, 0.15, . . . , 1.50 mm
Elutriation Constant	$K(0.00 \text{ mm}, t) = 1.0$/s
	$K(0.05 \text{ mm}, t) = 0.1$/s
	$K(0.10, 0.15, \ldots, 1.50 \text{ mm}, t) = 0.0$/s

$P_b(d, 0)$ to initialize the *a priori* estimate, X_0, we assigned the initial estimate error covariance matrix to be equal to the measurement error covariance matrix, i.e.,

$$P_{0,diag}(d_n, d_n) = R_{diag}(d_n, d_n, t) \tag{22}$$

Finally, we assumed that our idealized dynamic model was equally accurate across the spatial domain and had an intermediate accuracy relative to the linear measurement assignment, i.e.,

$$Q_{diag}(d_n, d_n, t) = 0.01 \tag{23}$$

Again, $n = 0, \ldots, 30$ and all off-diagonal terms are zero.

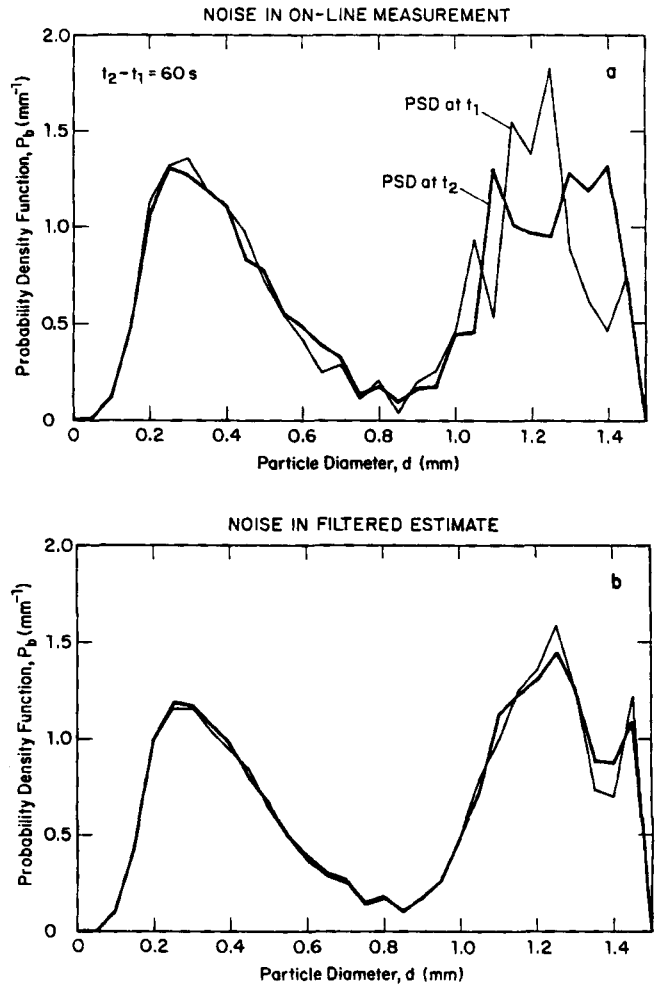

Figure 5. Comparison of noise in measurement and filtered estimate.

Results

The purpose of the experimental program was to demonstrate that the optimal filtering algorithm could yield an on-line, real-time, continuous, and well-behaved overall bed PSD estimate based on PSD measurements that are on-line and real-time but also somewhat corrupted with random error and available only at a discrete time interval of once every 60 s. In the experimental demonstration reported here, we produced the desired estimates throughout the course of a significant PSD transient.

As illustrated in Figure 4, we began the demonstration with a fluidized bed filled with an initial charge of fine-particle silica sand with distribution, $P_b(d, 0)$, and injected a fresh feed of large particles, $P_0(d)$, into the fluidized bed at a constant rate of approximately 0.045 kg/s. The dilution proceeded for a duration of over 2,700 s (45 min).

Figure 5 illustrates that the optimal filtering algorithm yields well-behaved estimates based on noisy measurements. Figure 5a shows two on-line measurements taken 1 min apart, with each measurement based on the raw sizing of 25,000 particles. These two measurements were selected to demonstrate the wild fluctuations that can occur in two successive on-line measurements. Figure 5b shows the filtered real-time estimates produced by the optimal filtering algorithm at the same two instances in time as the on-line measurements shown in Figure 5a. The measurement noise has been substantially eliminated in the real-time filtered estimate relative to the on-line PSD measurements.

Figure 6 illustrates the history of the dilution experiment. Presented in Figure 6a is the history of the on-line measurements during the dilution for measurement times $t = 0$, 900, and 2,700 s. This figure illustrates that PSD can be tracked experimentally by using only the discrete on-line measurements, and useful information can be obtained in spite of the jagged plot lines. Figure 6b illustrates the dilution history for the same time as in Figure 6a. Presented in this plot is the filtered real-time estimate, however. The improved behavior of the filtered estimate relative to the on-line measurement can be qualitatively appreciated from this comparison.

Recall that the PSD measurements and estimates are mathematically defined as probability density functions. As defined in Eq. 2, the PSD curves are normalized such that the area under them is 1.0. Figures 5 and 6 illustrate that the optimal filtering algorithm yields a smoothed estimate for the large-particle portion of the PSD curve (the portion that has the significant noise). One result of this smoothing appears to be that the area under the curve for the large particle portion has been increased. Consequently, the area under the small-particle portion of the curve must be reduced. This can be verified qualitatively. If we choose a particle diameter of 0.25 mm, and trace from plot 6a the value of the probability density function for time $t = 2{,}700$ s,

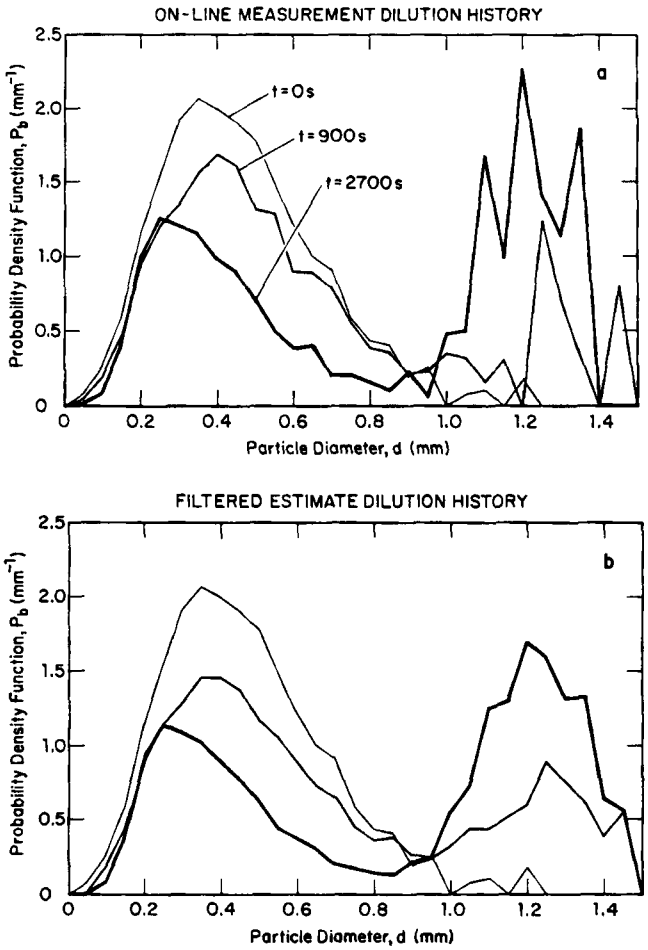

Figure 6. Comparison of dilution history for measurement and filtered estimate.

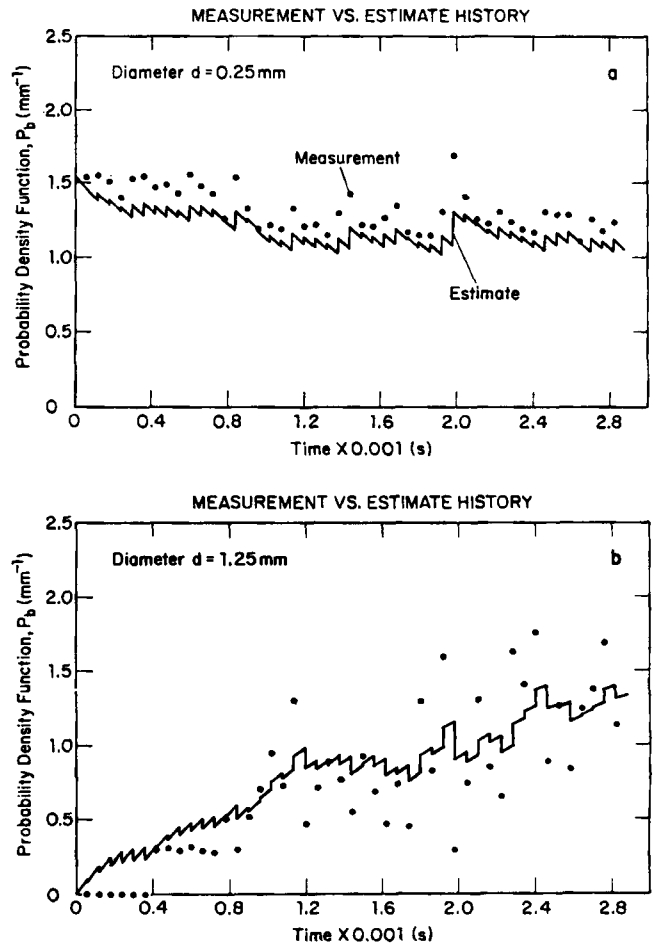

Figure 7. History of measurement vs. filtered estimate for small and large particle diameters.

we read a value of approximately 1.3 mm^{-1}. If we do the same on plot 6b, we read a value of approximately 1.1 mm^{-1}. Thus, we have verification that the peak of the curve for the small-particle portion has been lowered. Since the curve shape for the small-particle portion is nearly identical in both plots, we conclude that the area under it has been reduced.

In Figure 7 we present plots that depict the procedure outlined above, but with data that span the whole time of the dilution experiment. We stress that these plots present data that were produced over the course of the experiment. The on-line measurements were not first collected and then used to compute the filtered estimate. Rather, both the discrete-time measurements and continuous filtered predictions with updates as illustrated were produced in real time as delineated on the time axis.

In Figure 7a we compare the value of the probability density function for the discrete on-line measurements to the continuous filtered estimates for a particle diameter of 0.25 mm. Note that throughout the course of the dilution experiment the optimal filtered estimate is below the on-line measurement for this small particle diameter. We believe that this result is due to the area reduction for the small-particle range as described earlier.

Of particular interest is the result presented in Figure 7b. Here we consider data for a large particle diameter of 1.25 mm. At the earliest times during the dilution, the filtered estimate, "encouraged" by the idealized dynamic model, predicts that this large particle diameter is present in the fluidized bed. The on-line measurements contradict this prediction, however, and do not measure any particles of diameter equal to 1.25 mm until t = 420 s. But as the dilution proceeds, the filtered estimate is vindicated in that discrete on-line measurements begin to appear on either side of the filtered estimate. Toward the end of the dilution, the filtered estimate charts a continuous course through the noisy discrete-time measurements. This plot illustrates that the optimal filtering algorithm can produce a continuous estimate with significantly less random error relative to the on-line, discrete-time measurements.

Concluding Remarks

We have demonstrated that on a laboratory scale we can produce estimates of overall bed PSD that are on-line, real-time, virtually continuous, and well-behaved. Further, we have demonstrated that these estimates can be produced throughout the course of a significant distribution transient.

One aspect of optimal filter design that should not be underestimated is the development of the idealized dynamic model. The dynamic model is fundamental to the performance of the filtering algorithm. The use of an accurate model generally means that the filter will perform well.

Accurate models are sometimes difficult to obtain, however. Also, models that are comprehensive in their process description often lead to filtering algorithms that cannot be solved numerically in real time on the process computer available. Thus, assumptions are made to simplify and idealize the model. We note that some benefit still exists from employing optimal estimation theory when the model is not comprehensive in describing the process dynamics. At a minimum, the model should follow the correct direction of the dynamics most of the time. The determination as to the usefulness of a particular model relative to this admittedly vague criterion is left to the individual investigator.

Acknowledgment

The authors are grateful to the National Science Foundation, especially the Particulate and Multiphase Program of the Chemical and Process Engineering Division, for financial support of this work.

Notation

$\boldsymbol{A}$ = spatially discrete approximation of α
$\boldsymbol{B}$ = spatially discrete approximation of β
d = particle diameter, mm
d_{max} = maximum particle dia., 1.5 mm
F_0 = feed rate of solids to fluidized bed, kg/s
F_1 = overflow discharge rate of solids from fluidized bed, kg/s
F_2 = entrainment rate of solids from fluidized bed, kg/s
K = elutriation constant, 1.0/s; Eq. 3
N = number of diameters used in discrete approximation
$\boldsymbol{P}$ = PSD estimate error covariance matrix
$\dot{\boldsymbol{P}}$ = first time-derivative of $\boldsymbol{P}$, Eq. 13b
$\boldsymbol{P}_0$ = covariance matrix of $\boldsymbol{X}_0$, Eq. 12
P_0 = feed PSD probability density function, mm^{-1}
P_1 = overflow discharge PSD probability density function, mm^{-1}
P_2 = entrainment PSD probability density function, mm^{-1}
P_b = fluidized bed PSD probability density function, mm^{-1}
$\boldsymbol{Q}$ = covariance matrix of $\boldsymbol{U}$, Eq. 11a
$\boldsymbol{R}$ = covariance matrix of $\boldsymbol{V}$, Eq. 11b
t = time s
t_k = time of kth discrete measurement, s
$\boldsymbol{U}$ = noise vector representing uncertainty in the state model
$\boldsymbol{V}$ = noise vector representing uncertainty in the measurement model
w = weight of fluidized bed, kg
$\boldsymbol{X}$ = vector of N discrete fluidized bed PSD's, Eq. 8
$\dot{\boldsymbol{X}}$ = first time-derivative of $\boldsymbol{X}$, Eq. 9
$\boldsymbol{X}^*$ = optimal estimate of PSD
$\dot{\boldsymbol{X}}^*$ = first time-derivative of $\boldsymbol{X}^*$, Eq. 13a
$\boldsymbol{X}_0$ = *a priori* estimate of the fluidized bed PSD at initial time
$\boldsymbol{Z}$ = vector of discretized PSD measurements, Eq. 10b

Greek letters

α = dynamic PSD model coefficient, Eq. 6
β = dynamic PSD model coefficient, Eq. 7
δ = Dirac delta function.

Literature Cited

Ajinkya, M. B., "The Optimization and State Estimation of Distributed-Parameter Systems," Ph.D. Thesis, State Univ. of New York at Buffalo, 116 (1975).

Bryson, K. E., Jr., and Y.-C. Ho, *Applied Optimal Control,* Hemisphere, Washington, DC, 348 (1975).

Carnahan, B., H. A. Luther, and J. O. Wilkes, *Applied Numerical Methods,* Wiley, New York, 73 (1969).

Cooper, D. J., and D. E. Clough, "Experimental Tracking of Particle Size Distribution in a Fluidized Bed," *Powder Technol.,* in press, (1985a).

———, "Real-time Estimation of Dynamic Particle-Size Distributions in a Fluidized Bed: Theoretical Foundation," *AIChE J.,* **31,** 1,202 (1985).

Levenspiel, O., D. Kunii, and T. Fitzgerald, "The Processing of Solids of Changing Size in Bubbling Fluidized Beds," *Powder Technol.,* **2,** 87 (1968/69).

Ray, W. H., *Advanced Process Control,* McGraw-Hill, New York, 201 (1981).

Sage, A. P., and C. C. White, *Optimum Systems Control,* Prentice-Hall, Englewood Cliffs, NJ, 191 (1977).

Weimer, A. W., and D. E. Clough, "Dynamics of Particle Size/Conversion Distributions in Fluidized Beds: Application to Char Gasification," *Powder Technol.,* **26,** 11 (1980).

Wen, C. Y., and L. H. Chen, "Fluidized Bed Freeboard Phenomena: Entrainment and Elutriation, *AIChE J.,* **28,** 117 (1982).

Manuscript received Mar. 6, 1985, and revision received June 10, 1985.